Disentangling growth and decay of domains during phase ordering

Suman Majumder [*]

Amity Institute of Applied Sciences, Amity University Uttar Pradesh, Noida 201313, India

Using Monte Carlo simulations we study phase-ordering dynamics of a *multi*species system modeled via the prototype q-state Potts model. In such a *multi*species system, we identify a spin state or species as the *winner* if it has survived as the majority in the final state, otherwise, we mark them as *loser*. We disentangle the time (t) dependence of the domain length of the *winner* from *losers*, rather than monitoring the average domain length obtained by treating all spin states or species alike. The kinetics of domain growth of the *winner* at a finite temperature in space dimension $d = 2$ reveal that the expected Lifshitz-Cahn-Allen scaling law $\sim t^{1/2}$ can be realized with no early-time corrections, even for system sizes much smaller than what is traditionally used. Up to a certain period, all others species, i.e., the *losers*, also show a growth that, however, is dependent on the total number of species, and slower than the expected $\sim t^{1/2}$ growth. Afterwards, the domains of the *losers* start decaying with time, for which our numerical data appear to be consistent with a $\sim t^{-2}$ behavior. We also demonstrate that this approach of looking into the kinetics even provides new insights for the special case of phase ordering at zero temperature, both in $d = 2$ and $d = 3$.

I. INTRODUCTION

Existence of a discrete number of themodynamically degenerate ordered phases at low temperature is the characteristic of many phenomena, e.g., ordering of alloys, adsorbtion of atoms and rare gases on surface, phase transition in intercalation compounds [1–3]. Theoretically and computationally such systems can effectively be understood via a *multi*species model. In this context, the prototype is the q-state Potts model [4]. It has been used extensively, especially, to investigate phase transitions associated with such systems. Slight variation of the model makes it useful in diverse applications, be it in biological cell sorting or in modeling active matter systems [5–10]. In the context of phase transition, among all the studied problems one is particularly intriguing; to understand the nonequilibrium kinetics of approaching the final equilibrium state following a quench from an initial disordered state to a temperature below the transition temperature, where the equilibrium state is ordered. Such a process goes by the name of phase ordering or coarsening. Its dynamics is highlighted by the formation and growth of domains of like species [11,12]. The phenomenon is associated with the scaling of various functions that characterize its morphology, viz., the two-point equal-time correlation function exhibits a scaling of the form

$$C(r,t) = \tilde{C}[r/\ell(t)], \qquad (1)$$

where $\tilde{C}$ is a time (t)-independent master function, and $\ell(t)$ is the average linear domain size which is expected to grow as

$$\ell(t) \sim t^{\alpha}, \qquad (2)$$

with an exponent $\alpha = 1/2$, referred to as the Lifshitz-Cahn-Allen (LCA) law [13,14]. It turns out that $\alpha = 1/z$ where z is the equilbrium dynamical exponent [11].

Most of the simulation studies on phase-ordering dynamics of the Potts model were focused on estimating the value of α for $q \geqslant 2$. Early results for smaller system sizes at temperature $T > 0$, where no pinned or frozen dynamics was expected, showed that the exponent decreases from $\alpha = 1/2$ as q increases from $q = 2$ [15,16]. Later, using results from relatively larger system sizes for q as large as $q = 64$, it was shown that $\alpha = 1/2$ can only be realized in the long-time limit at subcritical temperatures [17–19]. However, for a square lattice the problem of presence of pinned configurations exists at low but finite temperatures [19,20]. On the other hand, due to the presence of pinned or frozen dynamics for $q \geqslant d + 1$, zero-temperature phase ordering is always of special interest both in $d = 2$ and 3 [13,15,21,22]. There, the domain growth is found to be significantly slower than the expected LCA law. For that matter, arguments in favor of logarithmic growth were also proposed [15]. In $d = 3$, even for the $q = 2$ Potts model which is basically the spin 1/2 Ising model, the issue of domain growth at $T = 0$ is not well settled [23–28]. In this regard, simulation studies of relatively larger system sizes even suggested a possible crossover in the domain growth from an early time $\sim t^{1/3}$ behavior to the asymptotic $\sim t^{1/2}$ behavior [28].

It must be clear by now that in phase ordering the primary quantity which one measures is the average linear size of the domains $\ell(t)$ as a function of time. Various morphology-characterizing functions can be used to provide a measure of $\ell(t)$. For example, it can be obtained from the decay of the two-point equal-time correlation function, or from the first moment of the structure factor, or from the first moment of the domain-length distribution function [11]. The measured $\ell(t)$

---

[*]smajumder.@amity.edu; suman.jdv@gmail.com

from different methods are proportional to each other. At this point it is worth noting that in phase ordering the dynamics is nonconserved, i.e., the global order parameter, viz., the magnetization, does not remain fixed to its starting value during the entire evolution following a quench. In other words, even though one typically begins with a uniform mixture of an equal number of every possible spin states or species, one eventually ends up with one of the spin states or species as the majority or *winner* in the final state. All other spin states or species which we refer to as *losers*, are present in negligible amount. So, it is easy to perceive that among all the spin states or species, domains of only the *winner* will always be growing before reaching the finite-size limit. Alongside, domain sizes of *losers* must be declining after a certain time and become almost vanishing in the final state. When one calculates the average domain length $\ell(t)$, this distinction of the spin states or species in terms of the *winner* or *losers* is not taken into account. Thus, the effect of decay of domains of *losers* is always embedded in the measured $\ell(t)$. Nevertheless, up to now, no attempts have been made to disentangle the kinetics of the *winner* from *losers*.

Here, keeping the above issue in mind, by means of Monte Carlo (MC) simulations we study phase-ordering dynamics of the q-state Potts model with a focus on monitoring the kinetics of individual spin states or species by categorizing them as the *winner* or *losers*. Our results for $2 \leqslant q \leqslant 10$ at a finite temperature for domain growth of the *winner* show no early-time correction to the expected scaling law. Apart from the growth of the *winner*, the kinetics of the *losers* exhibits a non-monotonic behavior with a long-time power-law decay. We also demonstrate that our approach of monitoring the kinetics of the *winner* provides improved results for the special case of phase ordering of the q-state Potts model at $T = 0$ in space dimension $d = 2$. Furthermore, in $d = 3$, for $q = 2$, which corresponds to the Ising model, we show that all the features that were expected to be observed in large systems can essentially be captured in a relatively much smaller system.

The remainder of the paper is organized in the following way. In Sec. II, we describe the model and details of the performed simulations. Then we present results in Sec. III, where we also describe the calculations of relevant observables. At the end in Sec. IV, we provide a brief summary, conclusion and outlook.

II. MODEL AND METHOD

The Hamiltonian of the q-state Potts model is given by

$$H = -J \sum_{\langle ij \rangle} \delta_{\sigma_i, \sigma_j}; \ \sigma_i = 1, 2, \ldots, q; \ J > 0, \quad (3)$$

where σ_i is the spin state or species type of the ith site, and the summation is over all possible pairs of nearest neighbors indicated by $\langle ij \rangle$. The model exhibits an order-disorder transition as a function of temperature. For $q = 2$, the Hamiltonian, represents a two-species system that differs from the Ising model Hamiltonian only by a factor of 2. For a square lattice, the corresponding transition temperature is $T_c = J/k_B \ln(1 + \sqrt{q})$, where k_B is the Boltzmann constant [4]. For $q \leqslant 4$ the transitions are second order whereas for $q > 5$ they are first order.

We study the model (3) by performing MC simulations on square and cubic lattices, respectively, for $d = 2$ and 3, with a linear size L along each Cartesian direction. We apply periodic boundary conditions in all possible directions. Dynamics in our simulations is introduced via Glauber spin-flip mechanism that changes the global concentration of each spin state or species during the evolution, and finally ends up with one of the spin states or species as the majority [29–31]. A typical spin-flip MC move consists of randomly choosing a site having the state σ_i followed by changing its state to any of the remaining $(q - 1)$ states. The move is then accepted in accordance with the standard Metropolis algorithm with a probability

$$p_i = \min[1, \exp(-\Delta E / k_B T)], \quad (4)$$

where ΔE is the change in energy due to the attempted move. L^d such attempts form a MC sweep (MCS) setting the unit of time.

To start our simulations, as initial condition we prepare a random mixture containing all possible (q) spin states or species in equal proportion, mimicking a high-temperature ($T = \infty$) paramagnetic or homogeneous phase. Such configurations are then quenched below the critical temperature T_c by fixing $T = 0.6T_c$. In our simulations, J/k_B sets the unit of temperature, and for convenience J and k_B are chosen to be unity. We also perform simulations at $T = 0$ where the criterion for the Metropolis update of the system gets simplified. There, an attempted move is accepted if $\Delta E \leqslant 0$. All the results presented are averaged over more than 100 independent realizations accounting for different starting configurations and thermal noise during evolution.

III. RESULTS

The results are presented in two subsections. In the first subsection, we discuss the results for $d = 2$ at the finite temperature $T = 0.6T_c$. In the other one, we present results for $T = 0$ in $d = 2$ and 3.

A. Phase ordering at finite T in $d = 2$

When a disordered system containing a homogeneous mixture of q spin states or species is quenched below T_c, it becomes unstable to fluctuations and starts evolving towards an ordered state where only one of the spin states or species survives as the majority. Snapshots for such an evolution using a square lattice at $T = 0.6T_c$ are presented in Fig. 1 for $q = 4$ and 10. In both cases the evolution commences with formation of domains of like spins as represented by the snapshots at $t = 10$ MCS. These domains then start growing with time, as evident from the snapshots at $t = 10^2$ MCS and $t = 10^3$ MCS, respectively, for $q = 4$ and 10. Afterwards, once the domains of individual spin state or species have attained a considerable size, one of the species keeps on growing further while the others start decaying and eventually almost vanish. This leads to the emergence of the *winner* species which stays as the majority in the final configuration. For example, in the case presented in Fig. 1, the yellow and purple states are *winners*, respectively, for $q = 4$ and 10. There all other states are marked as *losers*. By arranging the spin states or species
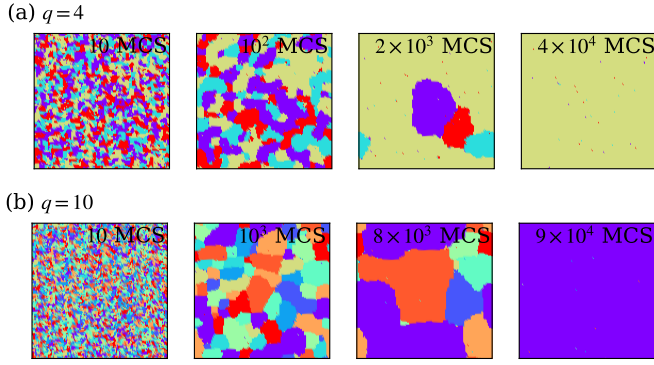
(a) $q = 4$

(b) $q = 10$

FIG. 1. Time evolution snapshots depicting the general sequence of events during phase-ordering dynamics of the q-state Potts model, at $T = 0.6T_c$ in $d = 2$ using a square lattice with linear size $L = 128$, for two different choices of q, as indicated. Different colors represent different spin states or species.
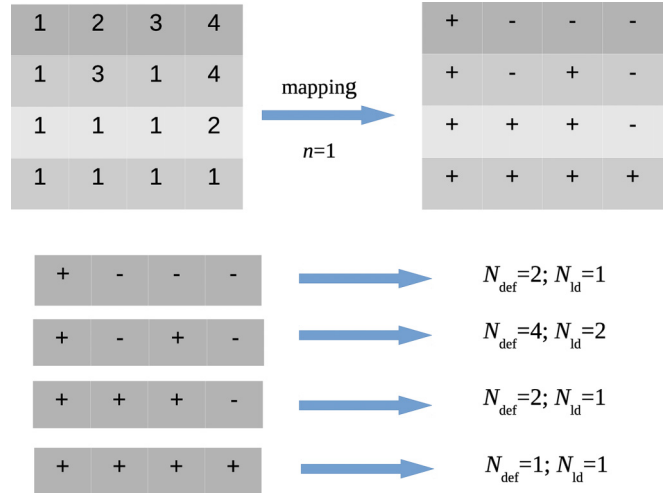

FIG. 2. The upper panel presents a schematic representing the mapping procedure from a typical $q = 4$ Potts lattice to an Ising-like lattice. The corresponding estimated number of defects N_{def} and number of linear domains N_{ld} of "+" spins are shown in the lower panel.

in descending order in terms of the total number of sites in the final configuration having that particular spin state or species, we assign a ranking n to them where

$$n \in \{1, 2, \ldots q\}. \tag{5}$$

The *winner* will have $n = 1$ and all other spin states or species with $n > 1$ correspond to *losers*. If a spin state has $n = q$, then it indicates that the number of sites in the final configuration belonging to that spin state or species is the least.

We start with measuring our primary quantity of interest, the growing characteristic length scale, which in the present case is the linear size of the domains. However, in contrast to the usual practice, we measure the length of the domains of each spin state or species as a function of time and store them during the simulation. The domain of an individual spin state or species is measured using a mapping of the Potts spins of every lattice site i to an Ising-like scalar variable as [32,33]

$$\psi_i^n = 2\delta_{\sigma_i,n} - 1; \quad n = 1, 2, \ldots q. \tag{6}$$

This gives a lattice of spin $\psi_i^n = \pm 1$ for every value of the Potts spin n. For example, the upper panel of Fig. 2 shows mapping of a 4×4 Potts lattice to the corrersponding Ising-like lattice for $n = 1$. By scanning through such lattices in x, y, and z (for $d = 3$) directions, we measure the total number of interfaces or defects N_{def} in each of the constituent Ising chains of the lattice, of course, by taking into account of the periodic boundary conditions. As a typical example, $N_{def} = 2$ and 1, respectively, for the first and last Ising chain shown in the lower panel of Fig. 2. Generally, in such an Ising chain, the total number of linear domains of "+" spin will be $N_{ld} = N_{def}/2$. In the case of percolating domains spanning throughout the lattice there will be Ising chains consisting of only "+" or "−" spins. In the former case we will consider it to be a single linear domain, i.e., $N_{ld} = 1$. For the latter case we will consider that there are no domains of "+" spins. The sum of size of domains of "+" spins obtained this way from all the constituent Ising chains of the mapped lattice must be equal to the total number N_+ of +1 spins present. Finally, the average linear size of domains of the spin state or species n

can be obtained as

$$\ell_n = \left\langle \frac{N_+}{\sum N_{ld}} \right\rangle, \tag{7}$$

where the $\sum$ is over all the Ising chains while scanning along any particular direction and $\langle \ldots \rangle$ indicates averaging over all possible directions. Thus, by using the corresponding Ising-like lattice for every spin state or species, we calculate the average linear size of domains of every spin state or species. Note that the subscript n in ℓ_n indicates the previously introduced ranking of the spin states or species. The average of domain lengths obtained from different trajectories are then calculated in terms of ℓ_n. Thus, from now onward ℓ_1 corresponds to the average linear domain size of the *winner* and ℓ_n with $n > 1$ correspond to *losers*. In the traditional way, different spin states or species are not distinguished, and average domain length ℓ at a given time is calculated by considering them alike, so that

$$\ell = \frac{1}{q_e} \sum_{n=1}^{q_e} \ell_n, \tag{8}$$

where $q_e \leqslant q$ is the total number of distinct spin states or species existing at that instance. The condition $q_e < q$ indicates that one or more of the spin states or species have vanished, most likely to happen at very late times.

Before proceeding further with the domain length for the *winner* and *loser*, we verify whether ℓ_1 satisfies the criterion of a scaling phenomenon (1). For that we calculate the two-point equal-time correlation function averaged over all the spin states or species as

$$C_{avg}(r, t) = \frac{1}{q} \sum_{n=1}^{q} \left[\langle \psi_i^n(t)\psi_j^n(t) \rangle - \langle \psi_i^n(t) \rangle\langle \psi_j^n(t) \rangle \right], \tag{9}$$

where r is the scalar distance between any two sites i and j. The scaling plots of $C_{avg}(r, t)$ by using $\ell(t)$ is presented in
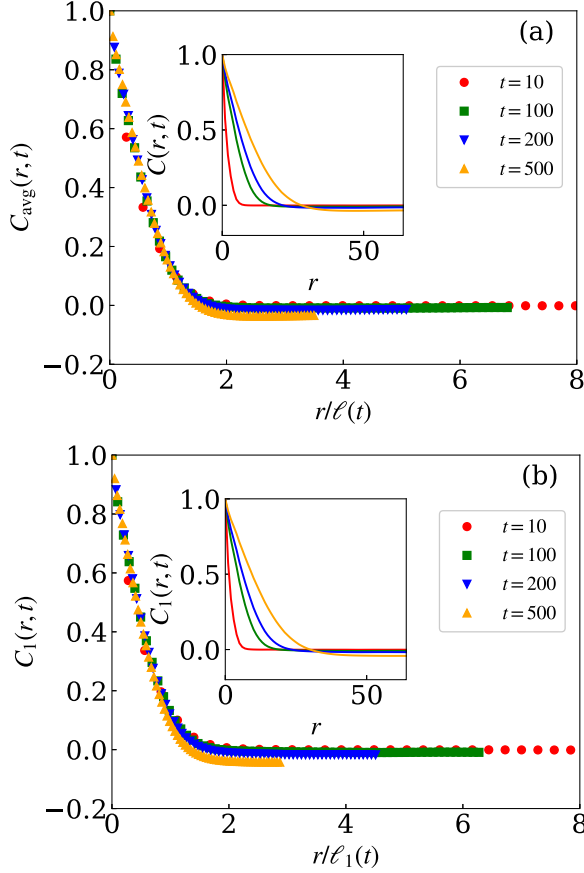
FIG. 3. Demonstration of fulfillment of the scaling criterion (1) of the two-point equal-time correlation function during phase ordering in a square lattice with $L = 128$ for $q = 4$, at $T = 0.6T_c$. In (a) the average linear domain length $\ell(t)$ is used as the scaling factor for the correlation function $C_{avg}(r, t)$, obtained from averaging over all the spin states or species. The same for the correlation function of the *winner* species $C_1(r, t)$, using the domain length of the *winner* $\ell_1(t)$ is shown in (b). The insets show the corresponding unscaled data at different times.

Fig. 3(a) for phase ordering in a square lattice system with $q = 4$ at $T = 0.6T_c$. The collapse of data for different times implies the fulfillment of the scaling criterion (1). Next, we calculate the two-point equal-time correlation function of the winner species

$$C_1(r, t) = \langle \psi_i^1(t)\psi_j^1(t) \rangle - \langle \psi_i^1(t) \rangle \langle \psi_j^1(t) \rangle, \qquad (10)$$

where ψ_i^1 is the Ising-like lattice variable introduced in Eq. (6) for $n = 1$, i.e., for the *winner* spin state or species. The corresponding scaling plots of $C_1(r, t)$ using the domain length of the *winner* $\ell_1(t)$ as the scaling factor, is shown in Fig. 3(b). Reasonably good collapse of data confirms the satisfaction of the required scaling criterion (1). In fact at early times, for small r the collapse of data in (b) is superior to the data presented in (a).

Having the fulfillment of a scaling phenomenon established, we move on to deal with time dependence of domain lengths in Fig. 4. There, the data for $\ell(t)$, obtained by considering all q spin states or species alike, show a much slower growth compared to the expected LCA law $\sim t^{1/2}$. Such an
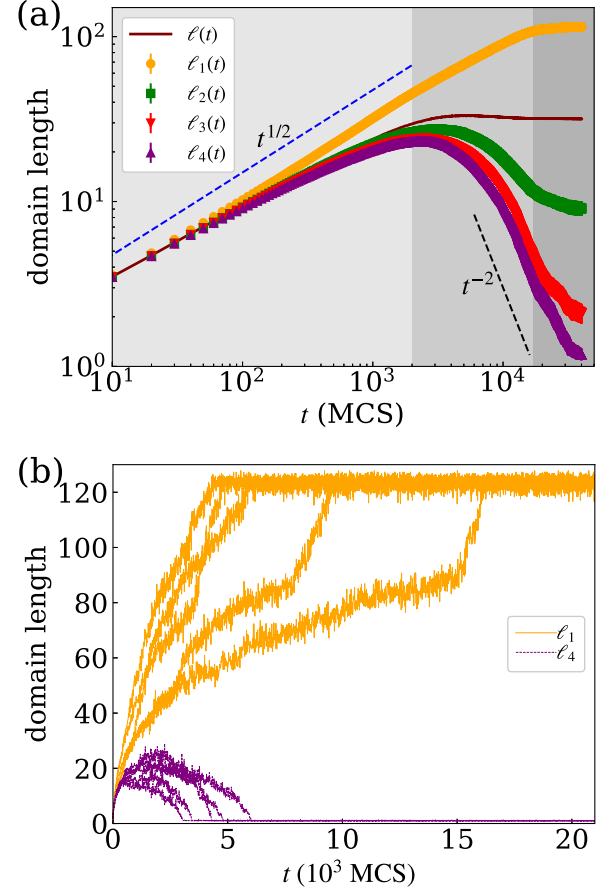

FIG. 4. (a) Double-log scale plots showing time dependence of different domain lengths for a phase-ordering system with $q = 4$ using a square lattice of linear size $L = 128$, at $T = 0.6T_c$. Here, $\ell(t)$ correspond to the traditionally calculated domain length obtained by averaging over all spin states or species. The other lengths presented are for different spin states or species in terms of their ranking using n (see text for details). According to the ranking, ℓ_1 corresponds to the domain length of the *winner* species and the rest are all *losers*. The dashed blue line represents the expected LCA growth $\sim t^{1/2}$. The dashed black line represents a power-law decay $\sim t^{-2}$. The shades in grey scale are introduced to roughly mark different regimes. (b) Domain lengths ℓ_1 and ℓ_4 vs. time on a linear scale for five different simulation runs for the same system as in (a).

inconsistency with the expected growth law has always been a problem for smaller system sizes, like $L = 128$, presented here. This could be explained via a combination of finite-time corrections and early advent of finite-size effects. In such cases, there have been attempts to extract the asymptotic growth by applying finite-size scaling via an ansatz considering an initial domain length [34–36]. However, the trend has always been to use larger system sizes to access larger length and time scales. As mentioned, we extract the time dependence of ℓ_n by categorizing the spin states or species as the *winner* or *losers*. The different domain lengths obtained this way are also plotted in Fig. 4. There, the data for domain length $\ell_1(t)$ of the *winner* show remarkable consistency with the expected $\sim t^{1/2}$ growth over an extended period starting from very early time. Followed by that it enters a regime where it still grows, however, with a smaller exponent. Finally,

it hits the finite-size limit and remains constant as long as we ran the simulations. The intermediate regime is essentially an extended crossover regime from the scaling regime to the finite-size limit. In contrast, the data for $\ell(t)$ show a much sharper crossover to the finite-size limit.

Intriguing is the behavior of the domain length of the *losers* as shown in Fig. 4 where data for ℓ_n with $n = 2, 3, \ldots q$ are plotted. In the scaling regime (lightest grey zone) they show a much slower growth compared to the *winner* or the expected LCA law. This slower growth is the root cause of the slower growth for $\ell(t)$ in the scaling regime. After the scaling regime, the growth of the *losers* gets seized for a very brief period, and eventually it enters into a decay regime that coincides with the intermediate crossover regime for $\ell_1(t)$. For ℓ_q, i.e., ℓ_4, the domain length of the last ranked spin state or species, the decay seems to be consistent with a $\sim t^{-2}$ behavior. This is subjected to further verification for other values of q, as will be done subsequently.

For $q > 2$, from von Neumann-Mullins law it is expected that domains will grow and shrink simultaneously depending on its number of sides or vertices [37,38]. However, it cannot be predicted that domains of which species will be the growing one. Although random, the species whose domain becomes percolating at the earliest, eventually becomes the *winner*. For the Ising model it has been shown that this happens soon after the quench from high temperature [39,40]. In Fig. 4(b), we present the time dependence of domain lengths of the *winner* ℓ_1 and *loser* ℓ_4 from five different simulation runs for the same system as in Fig. 4(a). In all cases it is observed that ℓ_4 starts decaying at a very early time suggesting that majority of the existing domains or clusters of the *loser* species are shrinking. On the other hand, ℓ_1 keeps on increasing monotonically. This implies that even though not all domains or clusters of the *winner* species may be growing, the percolating cluster is big enough to have the average domain size of the *winner* species showing a steady growth.

From now onward, we will consider ℓ_1 as the growing length scale to verify the expected scaling law for phase ordering in different cases. Additionally, we will investigate the behavior of domain lengths of the last ranked *loser*, i.e., ℓ_q. In Fig. 5(a), we compare the time dependence of $\ell_1(t)$ for $2 \leqslant q \leqslant 10$ using a square lattice of size $L = 128$ at $T = 0.6T_c$. Data for all q follow the expected $\sim t^{1/2}$ behavior for an extended period until they are affected by finite-size effects. Importantly, none of them show any early-time corrections. The amplitude of growth decreases as q increases. The same power-law growth with different amplitudes suggests that these growths can be quantified via a universal finite-size scaling function with a nonuniversal metric factor [33,41]. We have checked that an analogous plot using the average domain length $\ell(t)$ cannot provide the same universal picture for such a small system size.

The universality is not restricted to the behavior of $\ell_1(t)$ but gets reflected in the time dependence of $\ell_q(t)$ too, as shown in Fig. 5(b). There, $\ell_q(t)$ for all values of q exhibits a non monotonic behavior with first showing a growth followed by a decay. In the growth regime data for all q are almost parallel to each other. Albeit, the growth is much slower than the LCA law. Then, for all q there is a gradual crossover to the decay regime. There, at long time, the data are again parallel to each
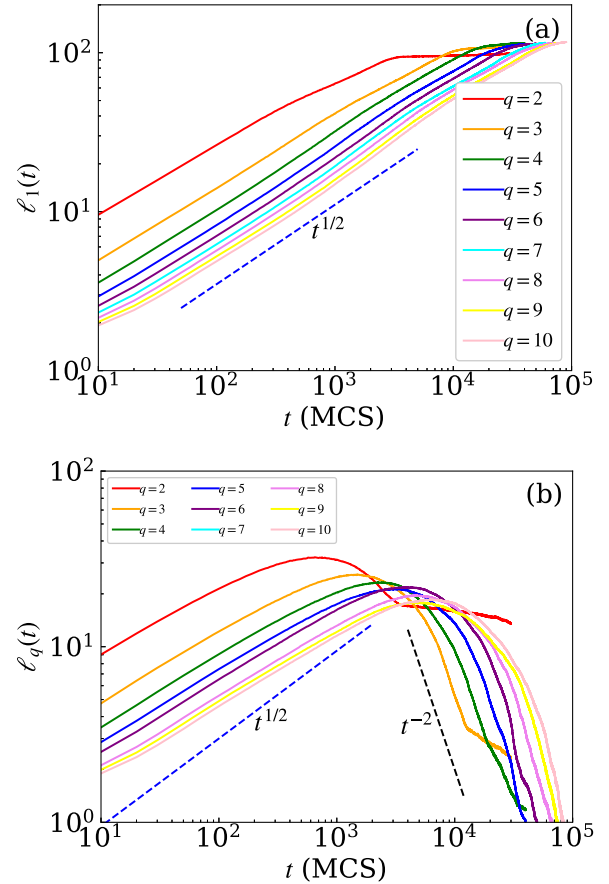

FIG. 5. Time dependence of the domain length of (a) the *winner* ℓ_1 and (b) *loser* ℓ_q for different values of q at $T = 0.6T_c$ using a square lattice system of size $L = 128$. The blue dashed lines represent the LCA growth law $\sim t^{1/2}$, and the black dashed lines represent the power-law decay $\sim t^{-2}$.

other, and are consistent with the $\sim t^{-2}$ behavior. One may thus be indulged to view it empirically as a power-law decay of the form

$$\ell_q(t) \sim t^{-z}, \tag{11}$$

where $z = 2$ is the dynamical exponent. However, we caution that the theoretical origin of the above relation and its validity at other possible conditions need to be checked.

We also check the system size dependence of the behavior of the domain lengths in Figs. 6(a) and 6(b), respectively, for the *winner* and *loser*. In (a) the data for $\ell_1(t)$ from different L follow each other until they enter the finite-size affected regime, and are consistent with the expected $\sim t^{1/2}$ behavior. In (b) too the data for smaller system sizes follow the larger ones up to a certain time, and then gradually start decaying. In the growth regime, data for all system sizes show a growth slower than the LCA behavior $\sim t^{1/2}$. In the decay regime all data are parallel to each other and are consistent with the empirical prediction in Eq. (11).

B. Phase ordering at $T = 0$ in $d = 2$ and 3

In the previous subsection we have established the usefulness of disentangling the growth of different spin states or species in terms of the *winner* and *losers*. Here, we explore

FIG. 7. Representative snapshots illustrating time evolution during phase ordering of the Potts model with (a) $q = 2$ and (b) $q = 4$ at $T = 0$ for a square lattice having $L = 128$. Again, different colors correspond to different spin states or species.
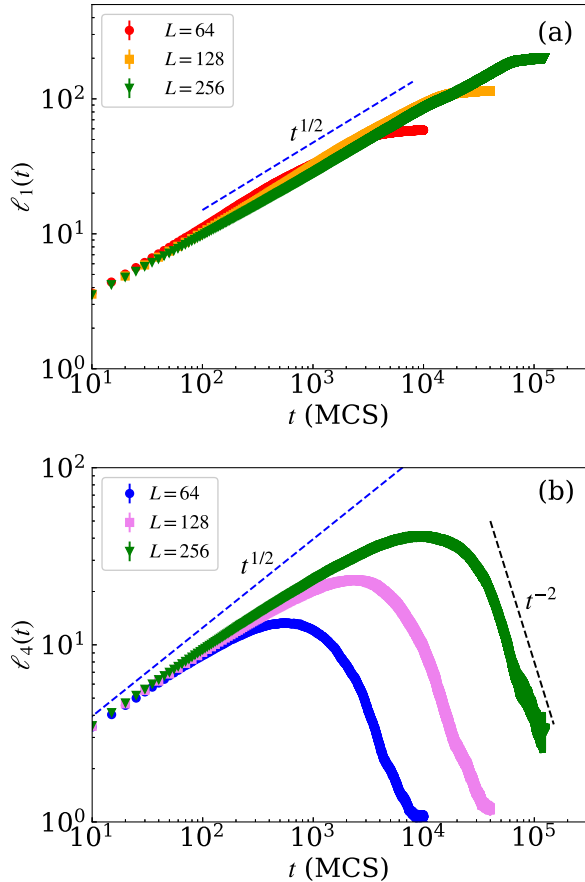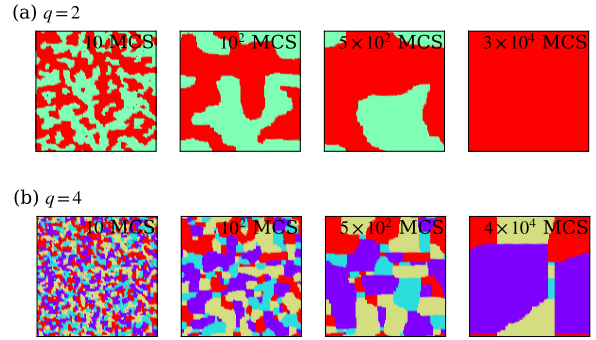

FIG. 6. System size dependence of the kinetics of domain length of (a) the *winner* and (b) *loser* for $q = 4$ at $T = 0.6T_c$. Square lattice system with three different L, as mentioned, are used. The dashed blue lines in (a) and (b) represent the LCA growth. The dashed black line in (b) represents a power-law decay $\sim t^{-2}$.

the same in investigating the special case of phase ordering in the q-state Potts model at $T = 0$ in $d = 2$ and also in $d = 3$.

1. $d = 2$

Phase ordering at $T = 0$ in $d = 2$ for $q = 2$ Potts model that corresponds to the Ising model, is the least challenging of all where one typically observes an ideal representation of the associated scaling law. There could be cases of dynamic freezing into stripped phases that may account for nearly 1/3 of the total simulation runs [42]. The rest of the simulations, however, reach the final ground state. A representative for time evolution of such a system using a square lattice of size $L = 128$ is shown in Fig. 7(a). The configuration at the latest time ($t = 3 \times 10^4$ MCS) corresponds to a typical ground state at $T = 0$, where only one of the spin states or species survives.

For larger q too, a significant fraction of total simulation runs get stuck. This observation is in accordance with the known difficulty of reaching ground states for $q \geqslant d + 1$ [13,15]. For a square lattice with higher q, a freezing fixed point corresponding to a stripped phase has been found [43,44]. For triangular lattice it has recently been observed that other interesting states like three-hexagon states and hexagonal tessellations with more than three clusters domi-

nate at $T = 0$ [45,46]. More importantly, it was argued that for $q \geqslant 3$ in $d = 2$ due the emergence of pinned configuration during the evolution, the system may get stuck in a disordered state leading to glassy dynamics [47–49]. Relatively recently, from long time simulations of the model it was further confirmed that for $q \geqslant 2$ in $d = 2$ the probability of reaching ground states is nonzero [22]. There, it was found that in the simulations where the system becomes static, the configuration has perfectly flat interfaces. In Fig. 7(b) where we present the evolution of the $q = 4$ Potts model, the snapshot at the latest time represents such a configuration with flat interfaces. Apart from these, at late time we too observed configurations which were evolving *ad infinitum*, as typically observed during phase ordering of the $d = 3$ Ising model at $T = 0$ [23,24]. We have also performed simulation for other values of q up to $q = 10$. The overall picture remains the same although the probability of reaching the ground state within our maximum simulation time almost vanishes as q increases, and episodes of observing pinned configuration become almost certain.

Having discussed the difficulties of reaching ground states, we move on to study the domain-growth kinetics at $T = 0$ by using our prescription of categorizing the different spin states or species as the *winner* and *losers*. Since for large q a significant fraction of the simulations do not reach the ground state, it is not straightforward to decide the *winner*. However, if one looks at the time evolution as in Fig. 7(b) for $q = 4$, then one can still choose the purple spin state or species as the *winner*, as it is the one that has been growing throughout, and has the largest domain size in the latest time. All the other spin states or species are thus considered to be *losers*. Following this we estimate all possible domain lengths, and present the corresponding plots for $q = 4$ in Fig. 8(a). There, we have also shown the data for the average domain length $\ell(t)$ obtained by the usual way of considering all spin states or species alike. The data for the *losers* and $\ell(t)$ clearly show a growth much slower than the LCA growth. The data for ℓ_4 in fact hint towards a power-law growth with an exponent $\alpha = 1/3$. On the other hand, the data for the *winner* again are fairly consistent with the $\sim t^{1/2}$ growth. Fitting with the form
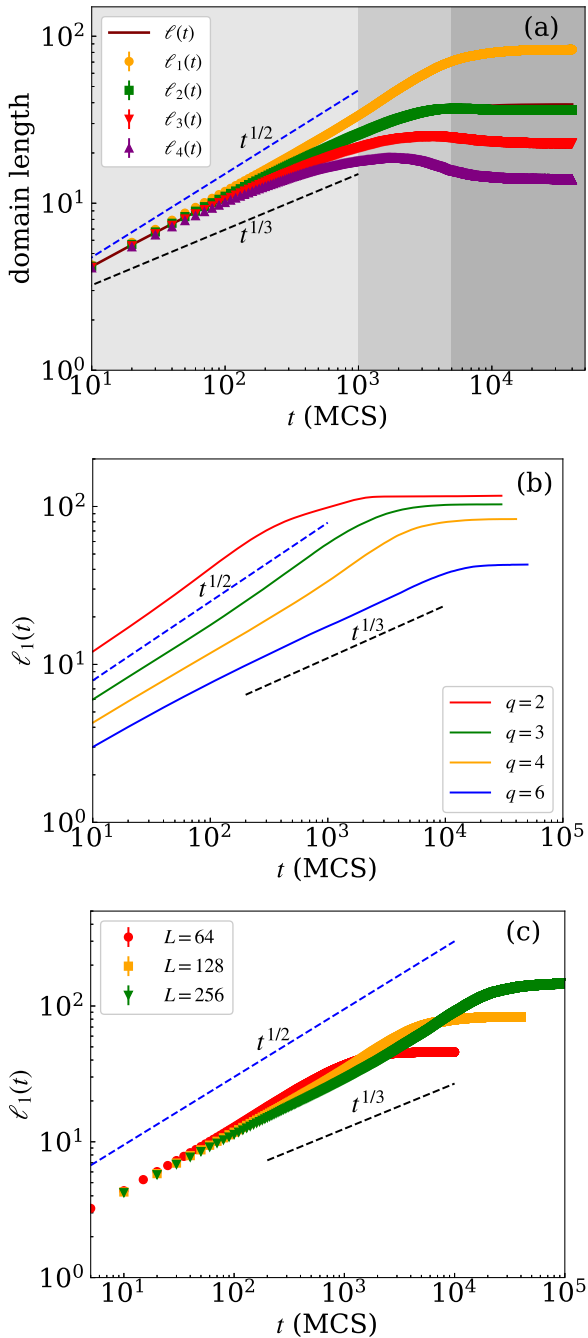
$$\ell_1(t) = At^\alpha, \tag{12}$$

FIG. 8. (a) Time dependence of measured domain lengths of the *winner* and *losers* in $d = 2$ for $q = 4$ during phase ordering at $T = 0$ using a square lattice with $L = 128$. The traditionally measured average domain length $\ell(t)$ is also plotted. (b) Domain length ℓ_1 of the *winner* species as a function of time for different values of q using the same square lattice. (c) System size dependence of $\ell_1(t)$ at $T = 0$ for $q = 4$. Dashed blue and black lines, respectively, represent the power-laws $\sim t^{1/2}$ and $\sim t^{1/3}$.

using the ranges $[10 : 3 \times 10^3]$, $[10^2 : 3 \times 10^3]$, and $[2 \times 10^2 : 3 \times 10^3]$, respectively, yield $\alpha = 0.453(1)$, $0.474(1)$, and $0.486(1)$. The slight deviation from $\alpha = 1/2$ is due to the presence of pinned configurations that do not allow the system to reach its ground state within the time period up to which we run the simulations. Nevertheless, our target here is

not to obtain the ground state, rather to apply our approach in quantifying the domain-growth kinetics with the data we obtain at $T = 0$ after running the simulations for a finite time. Hence, we abstain ourselves from performing simulation for longer times. Keeping in mind that the ground state is not reached always and looking at the long-time flat behavior of ℓ_4 in Fig. 8(b), Eq. (11) cannot be verified here.

In Fig. 8(b) we present the domain-growth kinetics of the *winner* species at $T = 0$ for different values of q. For $q \leqslant 4$ the growth is almost consistent with the expected LCA growth $\sim t^{1/2}$, until finite-size effects creep in. The data for $q = 6$ show significant deviation from LCA growth right from early time, and at later times the growth appears to be much slower. In fact the data seem to be consistent with the empirically drawn dashed line representing the power-law $\ell_1(t) \sim t^{1/3}$. This slow dynamics is a virtue of the fact that for larger q due to pinning effect the system gets stuck in metastable states. In the long time limit, the system can come out of the metastable state via merging of interfaces leading to an *avalanche*, i.e., rapid and drastic reorganization of domain structure [22]. The consistency of our data for $q = 3$ and 4 with the LCA law, suggests that encountering such metastable states during the evolution has negligible effect on the growth. We present the system size dependency of kinetics of ℓ_1 at $T = 0$ in Fig. 8 (c), which shows prefect consistency with the LCA growth for the smallest system size $L = 64$. For the largest system, i.e., $L = 256$, the data seem to be slightly deviating from the LCA growth, due to the slow dynamics arising from pinning effects. This suggests that pinning effects increase with system size.

It is evident from Fig. 8 that at $T = 0$, the value where ℓ_1 saturates at long t, does not approach the finite-size limiting value $\approx L$. This can be attributed to the same fact that at $T = 0$ not all the simulations could attain the ground state with all sites having the same spin states or species. Since this effect increases as q increases, one notices in Fig. 8 that the saturating value of ℓ_1 decreases as a function of q. To ignore the effect of the frozen dynamics, we now separate out the simulation runs where the *winner* species could achieve a length $\ell_1 \approx L$ until $t = 10^5$ MCS, which is significantly long for a system size as small as $L = 128$. The time dependence of ℓ_1 obtained only from the nonfreezed simulations are shown in Fig. 9 for different q. Again data for $q \leqslant 4$ are perfectly consistent with the LCA growth for an extended time period before encountering finite-size effects. In fact from a careful observation, one can appreciate the fact that the data are more consistent with LCA growth, in comparison with the data in Figs. 8. Although not apparent in the plot, the increasing estimated error on ℓ_1 as a function of q, is also a consequence of the fact that the fraction of nonfreezed simulations decreases as q increases.

In Fig. 9, one can also notice that for $q > 4$ at long times the growth of ℓ_1 seems to be faster than the LCA growth. For the largest q, i.e., for $q = 10$, apart from the long-time faster regime there exists an intermediate time period when the growth of ℓ_1 is extremely slow, consistent with a $\sim t^{1/4}$ be-havior. The slow phase corresponds to the presence of pinned configurations which eventually breaks via an *avalanche* leading to the long-time faster growth regime. For $q = 10$ the faster growth is apparently consistent with $\ell_1(t) \sim t^{3/2}$. Of course, since the pinning effect is smaller for small q, the
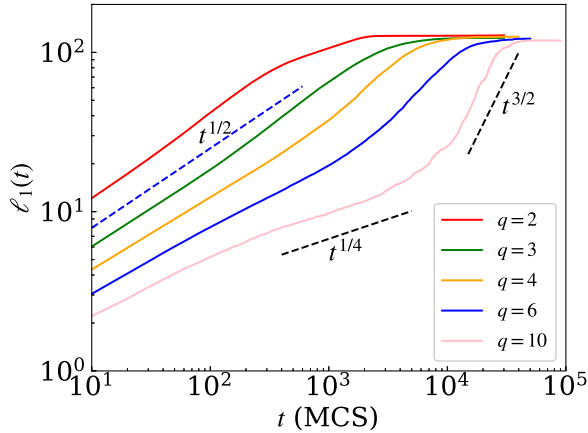
FIG. 9. Time dependence of the domain length ℓ_1 obtained from simulations which did not freeze within the maximum run time, at $T = 0$ in $d = 2$ for different q using a square lattice of linear size $L = 128$. The dashed blue and black lines represent possible power-law behaviors as indicated.

FIG. 10. Domain-growth kinetics in the $q = 2$ Potts model, i.e., the Ising model, in terms of domain lengths ℓ and ℓ_1, at $T = 0$ in $d = 3$. Data from simulations that did not get stuck are used. System used is a cubic lattice of length $L = 128$. Dashed lines with different colors correspond to different power-law behaviors as indicated. Different shades are guides to the eyes to distinguish different regimes.

slope of the faster-growth regime appears to be increasing as a function of q. A detailed study of even larger q values is needed to extract any functional dependence and limiting value of the exponent as a function of q during the *avalanche* of pinned configurations.

2. $d = 3$

After having an understanding of phase ordering in $d = 2$ at zero temperature, we now move on to explore the other special case of domain-growth kinetics in $d = 3$ at $T = 0$. Here, we restrict ourselves to the unique case of the $q = 2$ Potts model, i.e., the Ising model. For higher q one needs to perform rejection free MC simulations which we will present elsewhere.

The zero temperature phase ordering of the Ising model in $d = 3$ poses challenges because a major fraction of the simulations get stuck in local minima and thus one experiences frequent dynamic freezing. Hence, the measured time dependence of the average domain length deviates significantly from the expected LCA growth. In this regard, a dynamic crossover in the time dependence of the average domain length from a $\ell(t) \sim t^{1/3}$ at finite times to the asymptotic $\ell(t) \sim t^{1/2}$ behavior has been argued [50]. There the early-time $\ell(t) \sim t^{1/3}$ behavior was obtained from scaling argument using an analogy between diffusion of the domain walls with diffusion of a Rouse polymer [51]. There have been attempts to confirm this numerically by considering data only from simulations that did not get stuck [28]. Needless to say that simulations of larger system sizes were required to access large length scale and time scales in order to realize the aforesaid crossover to the universal LCA growth. In all these previous studies, however, the growth of the domains of the *winner* and *loser* were not disentangled. In Fig. 10, we present the kinetics of domain length of the *winner* for the $q = 2$ Potts model using a cubic lattice of $L = 128$, at $T = 0$ by considering only the simulations that evolved completely in the given maximum run time of our simulation, i.e., until $t = 4 \times 10^4$ MCS. There, we have also included the data for
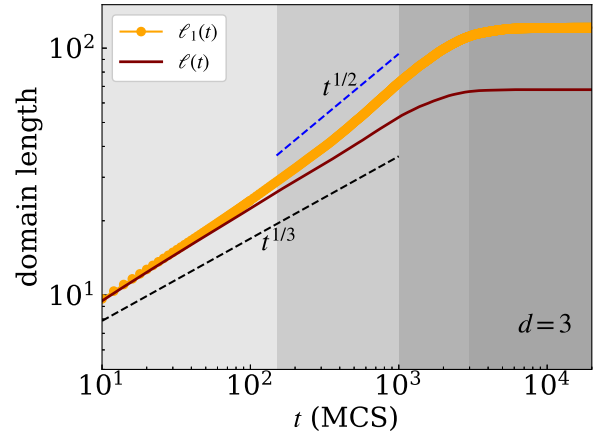
the average domain length $\ell(t)$ showing the presence of a single scaling law which is slower than $\ell(t) \sim t^{1/2}$, albeit, faster than $\ell(t) \sim t^{1/3}$. A fitting with the form (12) in the range $[10 : 200]$ yields $\alpha = 0.3703(3)$. On the other hand, $\ell_1(t)$ hints the presence of a crossover from a slower growth at early times to $\ell_1(t) \sim t^{1/2}$ behavior at long t. The early-time growth seems to be significantly faster than $\ell_1(t) \sim t^{1/3}$ behavior. Importantly, the crossover which was previously thought to be observed only at large length scale and time limit, is now realized much earlier in the behavior of ℓ_1, and for a much smaller system of linear size $L = 128$.

In view of the results for $T = 0$ in $d = 2$, presented in the previous subsection, for the $d = 3$ case too, one can expect the effect of pinned configurations. Thus, the crossover which is observed in Fig. 10 could supposedly be attributed to the pinning effect that stalls the dynamics for some time as the system gets stuck in metastable states. Later, it can come out of this metastable state via merging of interfaces leading to a rapid growth of domains that is referred to as an *avalanche*. To further substantiate this argument, in Fig. 11 we present the data of $\ell_1(t)$ from different system sizes for phase ordering with $q = 2$ at $T = 0$ in $d = 3$. In Fig. 11(a) we show the plot $\ell_1(t)$ obtained by considering all the simulations that we ran, irrespective of the fact whether it got stuck within the maximum allowed run time. The data for different system sizes nicely overlap with each other, and are in agreement with the presence of a single scaling law which seems to be slower than $\ell(t) \sim t^{1/2}$, but faster than $\ell(t) \sim t^{1/3}$. A fitting of the data for $L = 256$ using the form (12) in the range $[10 : 2 \times 10^3]$ provides $\alpha = 0.365(5)$. The corresponding plots using data considering only the simulations which could come out of the frozen dynamics within the given simulation run time is presented in Fig. 11(b). There, the data for the smallest system size $L = 64$ are perfectly consistent with $\ell_1(t) \sim t^{1/2}$ growth, with no indication of a crossover. While the absence of the crossover was expected as in previous studies using small system sizes, the realization of the LCA growth is contrastingly
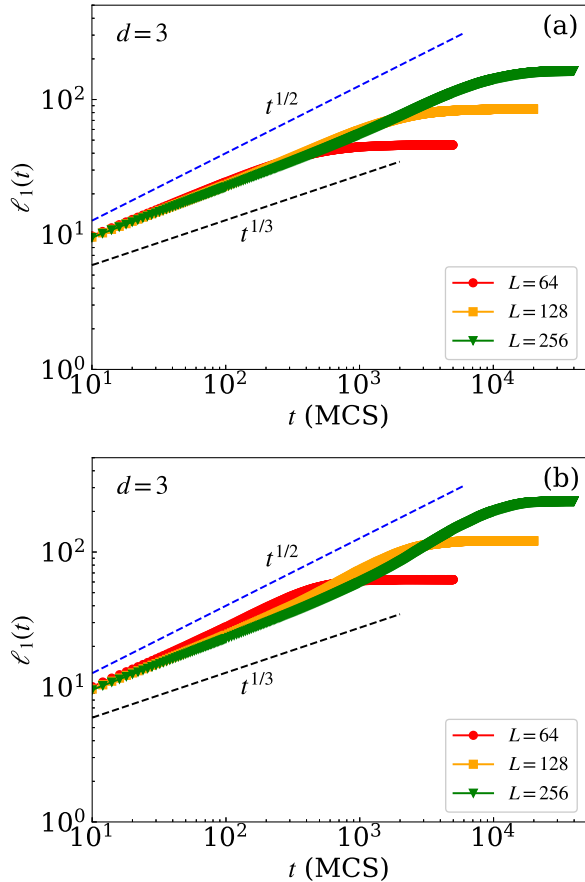
FIG. 11. System size dependence of domain-growth kinetics of the *winner* spin state or species for the $q = 2$ Potts model, i.e., the Ising model, in $d = 3$ at $T = 0$. In (a) we show the data including the runs where the dynamics got frozen, whereas (b) shows the data excluding them. In both figures dashed lines with different colors correspond to different power-law behaviors, as indicated.

surprising. In Fig. 11(b), as the system size increases one can notice the emergence of a crossover from an early-time slower growth to a faster one. However, the crossover time shifts as a function of L implying its system size dependence. This cannot be the case for a true crossover in the scaling. Thus, we infer that this is plausibly due to the effect of pinned configurations that stall the dynamics at finite times, and becomes more prominent as system size increases, similar to what we observed in the $d = 2$ cases for $q \geqslant 4$. The system comes out of this pinned dynamics in the form of an *avalanche* exhibiting a growth even faster than the LCA law. The data for the largest system size roughly indicate such a behavior in the postcrossover regime before hitting the finite-size limit. However, the exponent of the power-law seems to be smaller than 3/2 which we obtained for the case of $q = 10$ in $d = 2$ in Fig. 9.

IV. CONCLUSION

In summary, we have presented results from phase-ordering dynamics of a multispecies system modeled via the q-state Potts model in space dimensions $d = 2$ and 3. We have focused on disentangling the dynamics of different species on the basis of whether the species or spin state has survived as the dominating species in the final state. If the species is the majority one then we call it the *winner* or else *loser*.

In $d = 2$ at a finite temperature $T = 0.6T_c$, below the critical temperature T_c, we have observed that for $2 \leqslant q \leqslant 10$ the domain length ℓ_1 of the *winner* shows nice agreement with the expected LCA growth law $\ell_1(t) \sim t^{1/2}$ without any finite-time corrections for systems as small as a square lattice of linear size $L = 128$. This defies the usual tradition of using large system sizes. We have shown that such an observation with smaller system sizes cannot be realized if one uses the traditional average domain length $\ell(t)$ that is calculated by considering all spin states or species alike. We have also shown that the time dependence of the domain length of the *loser* exhibits a rich dynamical behavior. At early times the domains of the *loser* show a growth that is slower than the LCA growth. Followed by that it gradually starts decaying, and in the long-time limit exhibits a $\ell_q \sim t^{-2}$ behavior. To identify this as a universal behavior of the form $\ell_q \sim t^{-z}$, its validity needs to be verified in $d = 3$ and other physical conditions. In the same spirit, it would be interesting to further verify it for phase ordering in long-range interacting systems [52–54].

We have also explored the special case of phase ordering of the Potts model at $T = 0$ in $d = 2$. There, we have shown for $2 \leqslant q \leqslant 4$ that the time dependence of the domain length of the *winner* is consistent with LCA growth, provided one has separated the simulations which did not get stuck due to frozen dynamics. The time dependence of $\ell_1(t)$ for large q values show that at intermediate times the dynamics is stalled due to pinning. Subsequently, the system gets out of these pinned configurations which gets manifested in the form of an *avalanche* exhibiting an ultrafast domain growth. In the future, it would be worth to explore the scaling of the domain length in the *avalanche* regime for larger q. For that one needs to implement the rejection free n-fold algorithm for faster computation [55].

In $d = 3$, we have explored the special case of zero-temperature phase ordering for $q = 2$, i.e., for the Ising model. We have shown that if one examines the time dependence of ℓ_1, then the crossover in the growth from an early-time slower growth to a faster $\sim t^{1/2}$ growth can be realized in relatively smaller system size, e.g., in a cubic lattice of linear size $L = 128$. Using data from different system sizes we have shown that these crossover in growth is system size dependent. That poses a question about the true nature of the crossover. Rather, it indicates the presence of pinned dynamics which later is overcome in the form of an *avalanche* as observed for higher q in $d = 2$. Nevertheless, in this regard, again a detailed study in $d = 3$ for larger q is needed, which we take up as a future endeavor.

[1] D. E. Moncton, J. D. Axe, and F. J. DiSalvo, Neutron scattering study of the charge-density wave transitions in 2H–Ta Se$_2$ and 2H–Nb Se$_2$, Phys. Rev. B **16**, 801 (1977).

[2] A. N. Berker, S. Ostlund, and F. A. Putnam, Renormalization-group treatment of a Potts lattice gas for Krypton adsorbed onto graphite, Phys. Rev. B **17**, 3650 (1978).

[3] P. Bak and E. Domany, Theory of order-disorder transitions in the graphite intercalation compounds C$_8$Cs, C$_8$Rb, and C$_6$Li, Phys. Rev. B **20**, 2818 (1979).

[4] F.-Y. Wu, The Potts model, Rev. Mod. Phys. **54**, 235 (1982).

[5] F. Graner and J. A. Glazier, Simulation of Biological Cell Sorting Using a Two-dimensional Extended Potts Model, Phys. Rev. Lett. **69**, 2013 (1992).

[6] N. Chen, J. A. Glazier, J. A. Izaguirre, and M. S. Alber, A parallel implementation of the cellular Potts model for simulation of cell-based morphogenesis, Comput. Phys. Commun. **176**, 670 (2007).

[7] A. Szabó and R. M. H. Merks, Cellular Potts modeling of tumor growth, tumor invasion, and tumor evolution, Front. Oncol. **3**, 87 (2013).

[8] N. Guisoni, K. I. Mazzitello, and L. Diambra, Modeling active cell movement with the Potts model, Front. Phys. **6**, 61 (2018).

[9] S. Chatterjee, M. Mangeat, R. Paul, and H. Rieger, Flocking and reorientation transition in the 4-state active Potts model, Europhys. Lett. **130**, 66001 (2020).

[10] M. Mangeat, S. Chatterjee, R. Paul, and H. Rieger, Flocking with a q-fold discrete symmetry: Band-to-lane transition in the active Potts model, Phys. Rev. E **102**, 042601 (2020).

[11] A.J. Bray, Theory of phase-ordering kinetics, Adv. Phys. **51**, 481 (2002).

[12] S. Puri and V. Wadhawan (eds.), *Kinetics of Phase Transitions* (CRC Press, Boca Raton, FL, 2009).

[13] I. M. Lifshitz, Kinetics of ordering during second-order phase transitions, J. Exptl. Theoret. Phys. (USSR) **42**, 1354 (1962) [Sov. Phys. JETP **15**, 939 (1962)].

[14] S. M. Allen and J. W. Cahn, A microscopic theory for antiphase boundary motion and its application to antiphase domain coarsening, Acta Metall. **27**, 1085 (1979).

[15] S. A. Safran, Domain Growth of Degenerate Phases, Phys. Rev. Lett. **46**, 1581 (1981).

[16] P. S. Sahni, G. S. Grest, M. P. Anderson, and D. J. Srolovitz, Kinetics of the Q-State Potts Model in Two Dimensions, Phys. Rev. Lett. **50**, 263 (1983).

[17] P. S. Sahni, D. J. Srolovitz, G. S. Grest, M. P. Anderson, and S. A. Safran, Kinetics of ordering in two dimensions. II. Quenched systems, Phys. Rev. B **28**, 2705 (1983).

[18] K. Kaski, J. Nieminen, and J. D. Gunton, Domain growth and scaling in the q-state Potts model, Phys. Rev. B **31**, 2998 (1985).

[19] E. E. Ferrero and S. A. Cannas, Long-term ordering kinetics of the two-dimensional q-state Potts model, Phys. Rev. E **76**, 031108 (2007).

[20] M. Ibáñez De Berganza, V. Loreto, and A. Petri, Phase ordering and symmetries of the Potts model, Philos. Mag. **87**, 779 (2007).

[21] M. P. O. Loureiro, J. J. Arenzon, L. F. Cugliandolo, and A. Sicilia, Curvature-driven coarsening in the two-dimensional Potts model, Phys. Rev. E **81**, 021129 (2010).

[22] J. Olejarz, P. L. Krapivsky, and S. Redner, Zero-temperature coarsening in the 2d Potts model, J. Stat. Mech. (2013) P06018.

[23] J. Olejarz, P. L. Krapivsky, and S. Redner, Zero-temperature freezing in the three-dimensional kinetic Ising model, Phys. Rev. E **83**, 030104(R) (2011).

[24] J. Olejarz, P. L. Krapivsky, and S. Redner, Zero-temperature relaxation of three-dimensional Ising ferromagnets, Phys. Rev. E **83**, 051104 (2011).

[25] J. J. Arenzon, L. F. Cugliandolo, and M. Picco, Slicing the three-dimensional Ising model: Critical equilibrium and coarsening dynamics, Phys. Rev. E **91**, 032142 (2015).

[26] S. Chakraborty and S. K. Das, Fractality in persistence decay and domain growth during ferromagnetic ordering: Dependence upon initial correlation, Phys. Rev. E **93**, 032139 (2016).

[27] S. K. Das and S. Chakraborty, Kinetics of ferromagnetic ordering in 3D Ising model: How far do we understand the case of a zero temperature quench? Eur. Phys. J. Spec. Top. **226**, 765 (2017).

[28] N. Vadakkayil, S. Chakraborty, and S. K. Das, Finite-size scaling study of aging during coarsening in non-conserved Ising model: The case of zero temperature quench, J. Chem. Phys. **150**, 054702 (2019).

[29] R. J. Glauber, Time-dependent statistics of the Ising model, J. Math. Phys. **4**, 294 (1963).

[30] M. Newman and G. Barkema, *Monte Carlo Methods in Statistical Physics* (Oxford University Press, Oxford, 1999).

[31] D. P. Landau and K. Binder, *A Guide to Monte Carlo Simulations in Statistical Physics* (Cambridge University Press, Cambridge, 2014).

[32] S. K. Das and S. Puri, Dynamics of phase separation in multicomponent mixtures, Phys. Rev. E **65**, 026141 (2002).

[33] S. Majumder, S. K. Das, and W. Janke, Universal finite-size scaling function for kinetics of phase separation in mixtures with varying number of components, Phys. Rev. E **98**, 042142 (2018).

[34] S. Majumder and S. K. Das, Domain coarsening in two dimensions: Conserved dynamics and finite-size scaling, Phys. Rev. E **81**, 050102(R) (2010).

[35] S. Majumder and S. K. Das, Diffusive domain coarsening: Early time dynamics and finite-size effects, Phys. Rev. E **84**, 021110 (2011).

[36] S. K. Das, S. Roy, S. Majumder, and S. Ahmad, Finite-size effects in dynamics: Critical vs coarsening phenomena, Europhys. Lett. **97**, 66006 (2012).

[37] J. von Neumann, written discussion to Shape of metal grains, in *Metal Interfaces*, edited by C.S. Smith (American Society for Metals, Cleveland, Ohio, 1952) pp. 108–110.

[38] W. W. Mullins, Two-dimensional motion of idealized grain boundaries, J. Appl. Phys. **27**, 900 (1956).

[39] J. J. Arenzon, A. J. Bray, L. F. Cugliandolo, and A. Sicilia, Exact Results for Curvature-Driven Coarsening in Two Dimensions, Phys. Rev. Lett. **98**, 145701 (2007).

[40] T. Blanchard, F. Corberi, L. F. Cugliandolo, and M. Picco, How soon after a zero-temperature quench is the fate of the Ising model sealed? Europhys. Lett. **106**, 66001 (2014).

[41] W. Janke, S. Majumder, and S. K. Das, Universal finite-size scaling function for coarsening in the Potts model with conserved dynamics, J. Phys.: Conf. Ser. **2122**, 012009 (2021).

[42] V. Spirin, P. L. Krapivsky, and S. Redner, Fate of zero-temperature Ising ferromagnets, Phys. Rev. E **63**, 036118 (2001).

[43] J. Viñals and J. D. Gunton, Fixed points and domain growth for the Potts model, Phys. Rev. B **33**, 7795 (1986).

[44] J. Vinals and M. Grant, Role of activated processes and boundary conditions in the domain growth of the Potts model, Phys. Rev. B **36**, 7036 (1987).

[45] J. Denholm and S. Redner, Topology-controlled Potts coarsening, Phys. Rev. E **99**, 062142 (2019).

[46] J. Denholm, High-degeneracy Potts coarsening, Phys. Rev. E **103**, 012119 (2021).

[47] A. Petri, Lattice models of disorder with order, Braz. J. Phys. **33**, 521 (2003).

[48] M. J. de Oliveira, A. Petri, and T. Tomé, Crystal vs glass formation in lattice models with many coexisting ordered phases, Physica A **342**, 97 (2004).

[49] M.J. de Oliveira, A. Petri, and T. Tomé, Glassy states in lattice models with many coexisting crystalline phases, Europhys. Lett. **65**, 20 (2004).

[50] A. Lipowski, Anomalous phase-ordering kinetics in the Ising model, Physica A **268**, 6 (1999).

[51] P. E. Rouse, A theory of the linear viscoelastic properties of dilute solutions of coiling polymers, J. Chem. Phys. **21**, 1272 (1953).

[52] H. Christiansen, S. Majumder, and W. Janke, Phase ordering kinetics of the long-range Ising model, Phys. Rev. E **99**, 011301(R) (2019).

[53] W. Janke, H. Christiansen, and S. Majumder, Coarsening in the long-range Ising model: Metropolis versus Glauber criterion, J. Phys.: Conf. Ser. **1163**, 012002 (2019).

[54] H. Christiansen, S. Majumder, and W. Janke, Zero-temperature coarsening in the two-dimensional long-range Ising model, Phys. Rev. E **103**, 052122 (2021).

[55] A. B. Bortz, M. H. Kalos, and J. L. Lebowitz, A new algorithm for Monte Carlo simulation of Ising spin systems, J. Comput. Phys. **17**, 10 (1975).